

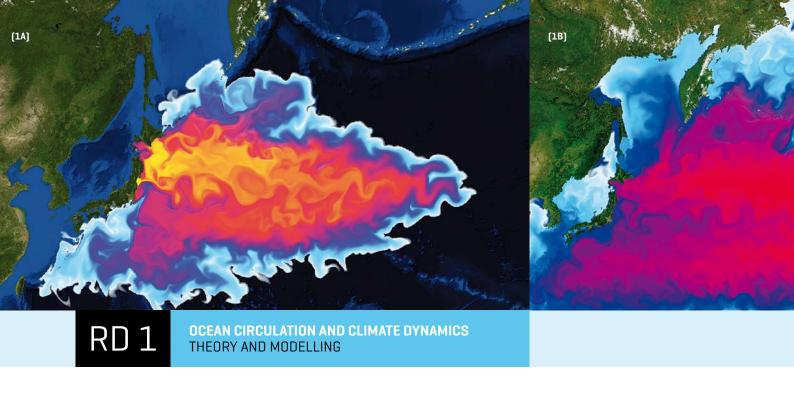


# GEOMAR Highlights 01

Scientific Highlights from the GEOMAR Research Divisions

		3		
			-	
(N)		3	-50	
	0	HAMMAN		
9				5
	HEN.			
	No.		4	
7	0	A Property of		
9.	-	The second	THE REAL PROPERTY.	

RD 1   The fate of <sup>137</sup> Cs released off				
Fukushima into the Pacific Ocean	04			
RD 1   Ventilation of the Equatorial Atlantic	06			
RD 2   The breath of the Ocean: Meteor cruise M91 to the upwelling off Peru	08			
RD 2   Does ocean acidification stimulate blue-green algal blooms in the Baltic?	10			
RD 2, RD 3   Evolution at the Sea - Marine Phyto-				
plankton can adapt to Ocean Acidification	12			
RD 2, RD 3   Sea urchin larvae in an acidified ocean – Understanding physiological tolerance mechanisms in sub-mm sized calcifying	9			
organisms	14			
RD 4   New insights into fluid flow				
in Hydrate Ridge, Oregon	16			
RD 4   Opening up the Red Sea	18			



## The fate of <sup>137</sup>Cs released off Fukushima into the Pacific Ocean

Erik Behrens, Franziska U. Schwarzkopf and Claus W. Böning, Joke F. Lübbecke (now at NOAA/PMEL, Seattle, USA)

The Fukushima Daiichi nuclear power plant accident triggered by the magnitude 9.0 Tõhoku earthquake and subsequent mega-tsunami on March 11, 2011 led to the discharge of unprecedented amounts of radioactive substances into the environment. A large fraction of this material entered the coastal waters off Fukushima, either through atmospheric deposition in the first days after the disaster or through the discharge of contaminated cooling waters. Among these radioactive substances are long-lived isotopes such as <sup>137</sup>caesium (<sup>137</sup>Cs) with a half life of ~30 years: how this contamination could spread over the Pacific Ocean in the next years has been studied by computer simulations with a high-resolution ocean model.

In the first weeks after the accident extremely high concentrations of short-lived (131 iodine with a half life of 8 days) and long-lived (137 caesium) radioisotopes were measured in samples of sea water and seabed sediments in the coastal area of Fukushima, raising concerns about damages to the local ecosystem, particularly through an accumulation of the long-lived substances in the food chain. Since 137 Cs is well soluble in sea water and the coastal waters are well-stirred by variable currents and tidal motions, it is expected that some portion of the radioactivity would swiftly be flushed away from the shelf region, and subsequently becoming dispersed over progressively larger areas of the Pacific Ocean. Recent measurements and modelling activities by international teams of scientists confirm these expectations (Aoyama et al. 2013, Tsumune et al. 2013)

An assessment of the possible long-term fate and dilution of the radioactive waters in the Pacific Ocean, was obtained by high-resolution model simulations at GEOMAR. A main requirement for obtaining reliable estimates of multi-year dispersion behaviors is a realistic representation of the strong current variability in the vicinity of the Kuroshio, implying a need to capture the characteristics of the mesoscale eddies, meandering currents and frontal systems in this area. This need was met with a dedicated, novel model configuration which utilized recent advances with a local grid refinement methodology, in which a global ocean model of "medium" resolution (average mesh sizes of ~40 km) was refined in the North Pacific sector to an "eddying"

mesh of ~8 km. Figure 1 displays a snapshot of simulated currents in the western North Pacific, indicating the rich detail of mesoscale features straddling the Kuroshio.

The spreading of radioactivity was simulated under the assumption that <sup>137</sup>Cs in sea water essentially behaves as a 'conservative' tracer or 'dye', dispersed mainly by the variable current fields, with biological processes being neglected. Since the exact discharge history of <sup>137</sup>Cs is still under investigation, some idealizations had to be made for the injection of this model 'dye' tracer; the main assumption being a constant release over a period of some weeks, with a total inventory of 10 PBq.

The long-term spreading and dilution of <sup>137</sup>Cs in the Pacific Ocean is illuminated in Figure 2. The initial spreading of the radioactivity is governed by vigorous eddies, leading to a fast dispersion and dilution in the western North Pacific. An interesting aspect is that the Kuroshio acts as a barrier for a southward penetration. After 1 year the tracer reached the dateline and the maxi-

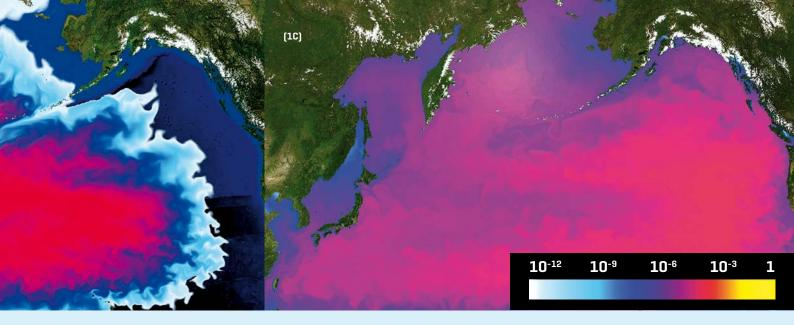


Figure 1: Temporal spreading of surface tracer concentrations after 6 months (1A), 2 years (1B) and 5 years (1C). Colour shading represents the concentration relative to the initial value after the release.

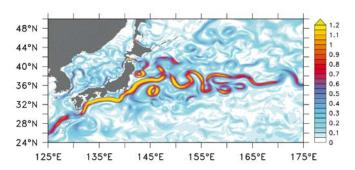


Figure 2: Snapshot of surface current speeds (m/s) in the eddy-resolving configuration  $(0.1^{\circ})$ 

mum concentrations had been diluted by 2 orders of magnitude compared to the initial values near Fukushima. Vertical mixing, especially during winter storms lead to a rapid dispersion of the tracer over the upper 500-600 m of the water column; interestingly, highest concentrations are then no longer been found at the surface, but in the main thermocline at depths of 200-300 m. In the following years the eastward spreading becomes more gradual due to the lower current speeds in the central and eastern North Pacific. While the bulk continues to head eastwards, parts of the tracer cloud begin to recirculate in southwestward direction, skirting the northern shores of the Hawaiian Islands, and another branch (with smaller concentrations) is invading the Bering Sea. About 2-3 years later the main tracer cloud reaches the North American coast, with a further dilution by 2 orders of magnitude; subsequently it separates in a northward and southward moving patch.

A prime conclusion from this simulation concerns the degree of mixing and dilution due the eddying currents in the ocean: with a dispersion of <sup>137</sup>Cs over nearly the whole ocean basin a few

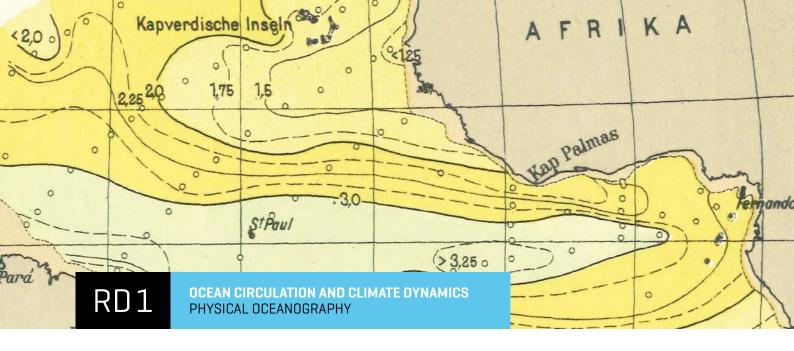
years after the accident, the radioactivity levels reaching the US coast can be expected to be much lower than those in the Japanese waters after the Fukushima disaster. A major caveat in the prediction of regional radioactivity values arises from the large uncertainties in the total inventory. Recent reconstructions indicated much higher (13 to 77 PBq) total inventories than the 10 PBq of <sup>137</sup>Cs assumed for this study: with these input values the peak radioactivity levels suggested by the model would be in the range of 13 to 77 Bq/m³ two years after the accident, and between 1 and 14 Bq/m³ after 4-7 years: this would be up to 10 times the pre-Fukushima values. The lack of knowledge about the total oceanic input after the accident, in conjunction with uncertainties about possible future discharges from the site, currently appears as main limitations for predicting future radioactive levels and their hazard potential.

#### References

Aoyama, M., Uematsu, M., Tsumune, D., & Hamajima, Y. (2013). Surface pathway of radioactive plume of TEPCO Fukushima NPP1 released 134Cs and <sup>137</sup>Cs. Biogeosciences, 10(5), 3067–3078. doi:10.5194/bg-10-3067-2013

Behrens, E., Schwarzkopf, F. U., Lübbecke, J. F., & Böning, C. W. [2012]. Model simulations on the long-term dispersal of <sup>137</sup>Cs released into the Pacific Ocean off Fukushima. Environmental Research Letters, 7(3), 034004. doi:10.1088/1748-9326/7/3/034004

Tsumune, D., Tsubono, T., Aoyama, M., Uematsu, M., Misumi, K., Maeda, Y., Yoshida, Y., et al. (2013). One-year, regional-scale simulation of <sup>137</sup>Cs radioactivity in the ocean following the Fukushima Daiichi Nuclear Power Plant accident. Biogeosciences Discussions, 10(4), 6259–6314. doi:10.5194/bgd-10-6259-2013



## **Ventilation of the Equatorial Atlantic**

#### Peter Brandt and Richard Greatbatch

The tropical Atlantic is characterized by the existence of extended oxygen minimum zones in both hemispheres separated by an equatorial oxygen maximum. This general distribution has been known since the first German Atlantic Expedition of 1925-27. Recently an ongoing deoxygenation became evident associated with declining minimum oxygen concentrations and expanding oxygen minimum zones. Although there is general scientific consensus that global warming might contribute to these oceanic changes, global models are not yet able to reproduce realistically the observed oxygen distribution or trend (Stramma et al. 2012). By combining a large dataset of shipboard and moored observations with idealized modeling, processes can be identified that are relevant for the establishment of the equatorial oxygen maximum and the resulting ventilation of the oxygen minimum zones from the equatorial band. Energetic equatorial mean and variable currents not resolved by global models are able to supply oxygen from the well-ventilated western boundary region towards the sluggish eastern tropical Atlantic (Brandt et al. 2012).

The oceanic oxygen distribution results from a subtle balance between ventilation and consumption. Oxygen is supplied to the ocean at the sea surface. It is transported downward by currents and mixing. Regions of strong currents are often associated with high oxygen concentrations as they often transport newly formed water masses originating at the sea surface. Oxygen consumption is generally found to be a maximum just below the near-surface layer, where large amounts of biological material are available for heterotrophic respiration. As consumption decreases strongly with depth, the vertical oxygen distribution in the tropical ocean is characterized by an oxygen minimum at intermediate depth (300 to 700m in the Atlantic), separating the well-ventilated near-surface layer from the oxygen-rich deeper layers. At intermediate depths within the low-oxygen layer, the climatological, time-averaged meridional oxygen distribution exhibits a broad maximum in the equatorial band separating

the oxygen minimum zones of both hemispheres (Figure 1). Poleward of the oxygen minimum zones, oxygen increases toward the subtropical gyres where the wind curl forces subduction of oxygen rich water masses into the intermediate water layers. This oxygen distribution of the Atlantic Ocean has been known since the German Meteor Expedition of 1925-27 exploring the tropical and South Atlantic between Africa and South America [Wattenberg, 1939] and ultimately led to the development of groundbreaking theoretical ideas about ocean ventilation. However, the simulation of a realistic oxygen distribution in global or basin-scale ocean models remains a challenge. This is partly due to the fact that the equilibrium

between ventilation and consumption in the sluggish flow regimes of the eastern tropical Atlantic is reached only after tens or hundreds of years and small inaccuracies have a strong impact on the equilibrated oxygen concentration. However, the main reason for the failure of coarse resolution models in simulating the equatorial oxygen distribution seems to be the absence of the mean and variable equatorial intermediate current system. At intermediate depths (300-700 m), the mean flow is composed of narrow zonal currents, including the westward flowing Equatorial Intermediate Current (EIC) centered on the equator between the eastward Southern and Northern Intermediate Countercurrents (SICC, NICC) located at about 2°S and 2°N, respectively. The mean eastward flow of the NICC and SICC has been recognized to ventilate the eastern tropical Atlantic by transporting oxygen-rich waters from the well-ventilated western boundary region towards the east. At the equator, the superposition of the

mean westward flow which carries low-oxygen water westward and interannually varying equatorial deep jets (EDJs) can result in intermittent flow reversals which also bring oxygen-rich water from the western boundary eastward.



Figure 2: Moored instruments are prepared for deployment during a research cruise. Typical moorings in the oxygen minimum zone or near the equator contain an ADCP (white cylinder with transducers to the left), temperature, salinity and oxygen sensors (in the cage, middle-left), and buoyancy elements that hold the mooring upright in the water column (yellow and orange balls).

During recent years, within the framework of the Collaborative Research Centre (SFB) 754 "Climate-Biogeochemistry Interactions in the Tropical Ocean", a large number of research cruises have been carried out in the tropical North Atlantic. During these cruises oxygen was measured on-station with a CTD/O2 probe and velocity was acquired continuously using the shipboard Acoustic Doppler Current Profilers (ADCPs). Additionally, time series from moored instrumentation (Figure 2) were collected from the equatorial region showing substantial variability on interannual time scales (Figure 3). To test the hypothesis that the observed oxygen distribution is influenced to first order by the ventilation due to the mean and variable equatorial current system, an advection-diffusion model was applied that includes an oxygen source in the western boundary region and oxygen consumption elsewhere. Giving the model a velocity field resembling what we know of the circulation in the tropical Atlantic at 500 m depth leads to an equilibrium oxygen distribution that includes oxygen minimum zones in both hemispheres separated by a region of elevated oxygen in a band about the equator (Figure 3). Such idealized simulations help to understand the ventilation processes responsible for the mean oxygen distribution and, at the same time, give hints about the consequences of changes in the strength of different ventilation processes for the oxygen concentration and distribution in the future.

#### References

Brandt, P., R. J. Greatbatch, M. Claus, S.-H. Didwischus, V. Hormann, A. Funk, J. Hahn, G. Krahmann, J. Fischer, and A. Körtzinger [2012], Ventilation of the equatorial Atlantic by the equatorial deep jets, J. Geophys. Res., 117, C12015, doi:10.1029/2012JC008118.

Stramma, L., A. Oschlies, and S. Schmidtko [2012], Mismatch between observed and modeled trends in dissolved upper-ocean oxygen over the last 50 yr, Biogeosciences, 9, 4045-4057, doi:10.5194/bq-9-4045-2012.

Wattenberg, H. (1939), Die Verteilung des Sauerstoffs im Atlantischen Ozean, Deutsche Atlantische Expedition Meteor 1925–1927, vol. 9, 132 pp., De Gruyter, Berlin.

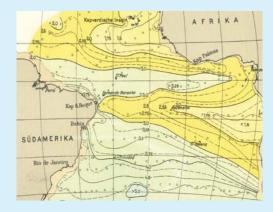


Figure 1: Oxygen distribution [cm³l-¹] in the Atlantic Ocean at 600 m depth obtained during the first Meteor expedition in 1925-27. Yellow regions mark the tropical oxygen minimum zones of both hemispheres separated by the equatorial oxygen maximum marked by greenish colors [from Wattenberg 1939].

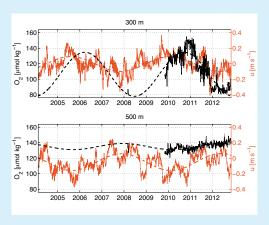


Figure 3: Time series of zonal velocity (solid, red) and oxygen (solid, black) from moored observations at the equator, 23°W at 300 m (middle panel) and 500 m (lower panel) reveal interannually varying EDJs; dashed curves are 4.5-year harmonic fits (update from Brandt et al. 2012).

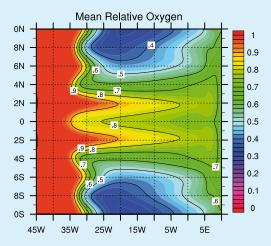
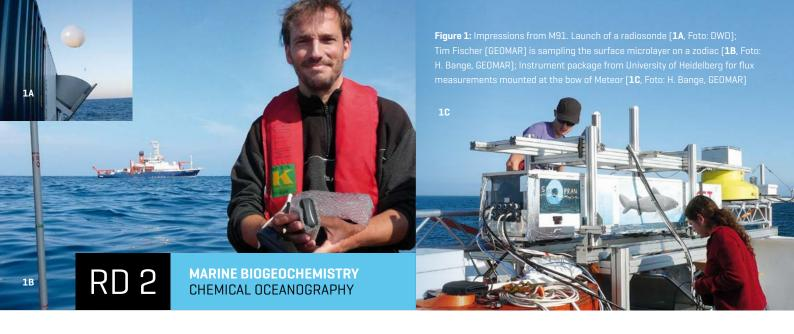


Figure 4: Mean relative oxygen concentration as simulated with the advection-diffusion model using a mean velocity field resembling that of the tropical Atlantic at 500 m depth and equatorial deep jets oscillating at a period of about 4.5 years (from Brandt et al. 2012).



### The breath of the Ocean

Meteor cruise M91 to the upwelling off Peru

Hermann W. Bange, Annette Kock, Damian L. Arevalo Martinez and the Team of M91

The overall goal of the Meteor cruise M91 (December 2012) was to conduct an integrated biogeochemical study on the Peruvian upwelling and the adjacent OMZ in order to assess their importance for the production and emissions of climate-relevant trace gases. M91 was funded by the German BMBF project SOPRAN (Surface Ocean Processes in the Anthropocene) as German contribution to the international SOLAS (Surface Ocean – Lower Atmosphere Study).

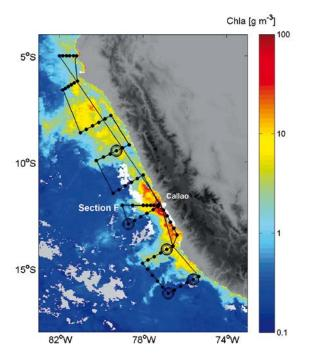
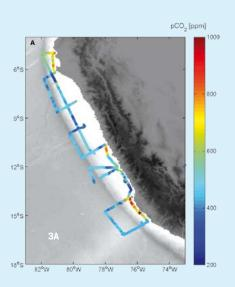


Figure 2: M91 cruise track and MODIS Aqua mean chlorophyll a concentrations during December 2012. Five 24h stations were conducted during M91; their positions are marked with circles. Monthly mean chlorophyll a concentrations were obtained from http://oceandata.sci.gsfc.nasa.gov/MODISA/Mapped/Monthly/4km/chlor/.

The world's oceans play an important role in the global biogeochemical cycles of carbon, nitrogen and sulphur. It is not too surprising that many climate relevant trace gases are originating as intermediates or by-products of various microbiological processes in the marine environment. A significant fraction of biological productivity in the ocean depends on the concurrent availability of nutrients and lights and is, therefore, restricted to the euphotic zone (i.e. the small sunlit upper part of the ocean water column). While light is usually available throughout the year in the eastern South Pacific (ESP), nutrient (i.e. nitrate and phosphate) concentrations are extremely depleted in large parts of the surface layer. Nutrient availability and, thus, the productivity of the ESP depend on physical processes which inject nutrients into the upper ocean layer.

The coastal region off Peru belongs to the four major eastern boundary upwelling systems. Here, steady winds blowing parallel to the Peruvian coast are the reason for the westward movement of the upper water masses which are replaced by nutrient-rich subsurface water masses triggering massive phytoplankton blooms. Therefore, the Peruvian upwelling region is one of the most productive regions of the global ocean. The high biological production, in turn, leads to a high flux of organic material out of the euphotic zone to the subsurface ocean where it is respired with oxygen by microorganisms resulting in a zone with extremely depleted oxygen concentrations (the so-called oxygen minimum zone, OMZ). Since the production of trace gases such as carbon dioxide, nitrous oxide, methane, dimethyl sulphide and others are either depending on phytoplankton or oxygen-sensitive microbial processes, the Peru upwelling and the adjacent OMZ seem to be ideal sites for trace gas cycling. However, the importance of the Peru upwelling for the production and atmospheric emissions of climate relevant traces is largely unknown.

To this end, the R/V Meteor cruise M91 to the upwelling off Peru was conducted within the framework of the BMBF-funded project SOPRAN (Surface Ocean Processes in the Anthropocene; www.sopran.pangaea.de). M91 is a contribution to the SOLAS



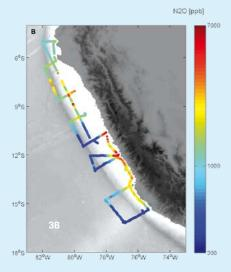


Figure 3: Surface distribution of  $CO_2$  (3A) and  $N_2O$  (3B) during M91. Please note the logarithmic scaling of the  $N_2O$  measurements.

(Surface Ocean — Lower Atmosphere Study, www.solas-int.org) midterm strategy initiative "Air-sea gas fluxes at eastern boundary upwelling and oxygen minimum zones system". M91 took place from 01 to 26 December 2012. 24 scientists from various SOPRAN subprojects as well as three scientists from the Instituto del Mar del Perú (IMARPE, Callao) and two scientists from the Joint Collaborative Centre SFB754 (Kiel) participated in the cruise. The major objectives were (i) to quantify the emissions of traces gases such as nitrous oxide (N2O), carbon dioxide (CO2) halocarbons (e.g. bromoform, methyl iodide), dimethyl sulphide, volatile organic compounds and other trace gases from the upwelling region and the deposition of aerosols to the ocean, (ii) to investigate the role of the seasurface microlayer for the exchange of trace gases across the ocean/atmosphere interface and (iii) to investigate the role of the coastal upwelling and the underlying OMZ off Peru as a source of trace gases. The various work packages of M91 included in-situ measurements of atmospheric and dissolved trace gases, aerosols, nitrogen cycle processes and nitrogen isotopes in the water column, dissolved organic matter in the surface microlayer, upwelling velocity and exchange fluxes across the ocean/atmosphere interface (Figure 1).

Eight transects perpendicular to the Peruvian coast located between 5°S and 16°S have been sampled (Figure 1). In addition, we sampled the coastal time series stations off Callao (Section F) and a transect parallel to the Peruvian coast south of Callao. Moreover, five 24h-stations, where the ship stayed at one position for 24h, were performed. In total, 123 radiosonde launches, 98 CTD/Rosette and 55 microstructure casts as well as 45 sampling trips with a zodiac were performed. Continuous underway atmospheric and surface ocean sampling and measurements were performed along the entire cruise track.

First results from M91 are presented in Figures 2 and 3: Chlorophyll a concentrations were very high in the narrow band of upwelling along the Peruvian coast (Figure 2). The massive phytoplankton blooms are resulting from nutrient-rich subsurface waters which are brought to the surface during the upwelling

at the shelf. Mesoscale circulation structures (so-called eddies), which are a common feature of the ESP, result in a transport of chlorophyll-rich surface waters away from the coast towards the open ocean. This is clearly visible as the ring-like structures of high chlorophyll in Figure 2.

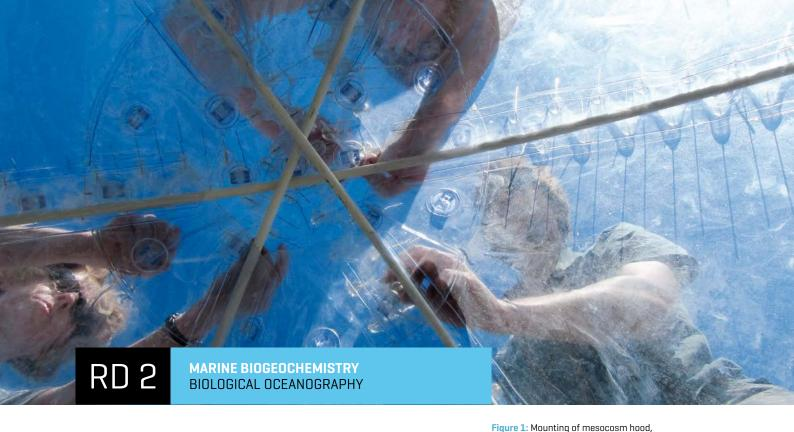
The surface distributions of dissolved carbon dioxide ( $CO_2$ ) and nitrous oxide ( $N_2O$ ) are shown in Figure 3. Measurements were performed with a novel combined analyser system, which was set up at GEOMAR, allowing combined measurements of dissolved and atmospheric mixing ratios of  $N_2O$  and  $CO_2$  with unprecedented high sampling frequency and precision. With this continuously operated underway system even small scale variabilities of  $N_2O$  and  $CO_2$  in the surfaces waters off Peru could be detected. We measured extremely high  $pN_2O$  and  $pCO_2$ . In the case for  $N_2O$  these are the highest surface concentrations ever measured in the surface ocean. In general, the partial pressures of both  $N_2O$  and  $CO_2$  are associated with sites of high chlorophyll in the upwelling along the coast. However, the maxima of  $pN_2O$  and  $pCO_2$  do not appear concurrent at the same coastal upwelling sites indicating that other local effect may also be important.

During the next six months the majority of the measurement from M91 will be finalized. An international M91 data workshop is planned for March 2014 and by then we hope to be able to draw a comprehensive picture of trace gas emissions from of the upwelling off Peru where the ocean is taking a breath and exhaling trace gases.

#### **Acknowledgments**

M91 is a joint effort of GEOMAR (Kiel), DWD (Hamburg), IOW (Warnemunde), IMARPE (Callao, Peru), LDEO (Palisades, NY), MPI for Chemistry (Mainz), RSMAS (Miami, FL), TUB (Braunschweig), U Bremen, UEA (Norwich, UK), U Hamburg, U Heidelberg, U Kiel, and U Massachusetts (Dartmouth, MA). M91 is funded by SOPRAN (Surface Ocean Processes in the Anthropocene) through BMBF grant # FKZO3F0611A.





## Does ocean acidification stimulate blue-green algal blooms in the Baltic?

Autor: Ulf Riebesell for the KOSMOS 2012 team

While many groups of marine organisms may suffer from ocean acidification, in particular those that build their shells and skeletons of calcium carbonate, some groups may benefit from increasing seawater acidity. Among them could be the blue-green algae, which inhabit all regions of the world ocean. As blue-greens are not the ordinary phytoplankton, changes in their productivity may have far-reaching implications for marine food webs and biogeochemical cycles.

Blooms of blue-green algae, also called cyanobacteria, pop up in the Baltic Sea every summer. As some members of this group can produce toxins, their mass occurrences can be quite harmful. They are also believed not to be a preferred food for the herbivorous zooplankton, which may be part of the reason why they can accumulate in massive amounts. Cyanobacterial blooms can cover almost the entire Baltic Sea Proper (Figure 3) and can become a nuisance to tourists enjoying

Foto: Silke Lischka, GEOMAR

Laboratory experiments indicate that cyanobacteria are among the winners of ocean acidification. They don't seem to be bothered much by increasing seawater acidity, but they benefit from elevated CO2 levels. The reason for this may be found in their evolutionary history. Blue-greens are ancient - they were the first to inhabit our planet and are considered responsible for

creating the oxygen in our early atmosphere. In those days CO<sub>2</sub>

the pleasures of beach-life along the Baltic Sea coastlines.

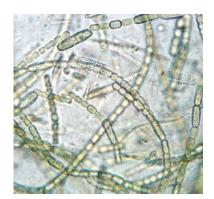


Figure 2: Cvanobacterium Aphanizomenon flos-gauge collected from the mesocosm.

levels were far higher than at present, which made it easy for them to acquire CO2 for photosynthesis. CO2 levels have declined dramatically since those early days and cyanobacteria had to learn utilizing this essential resource at much lower concentration. They did, but other groups of phytoplankton which evolved more recently found more clever ways of drawing inorganic carbon from seawater. While many of these seem to profit little from increasing CO<sub>2</sub> levels, because they are already quite efficient in doing so, cyanobacteria do. Increasing CO2 concentrations may therefore play out to their advantage, raising the

Foto: Ulf Riebesell, GEOMAR

The answer to this question would be no big deal if cyanobacteria were just the ordinary phytoplankton - one phytoplankton group thriving at the expense of another. But cyanobacteria are unique. Members of this group are the only or-

question whether the future ocean will experi-

ence a rise in cyanobacterial productivity.

ganisms capable of fixing molecular nitrogen into ammonia. As such this group is critically important in replenishing the pool of bioavailable nitrogen in the ocean, a pool that is continuously diminished by denitrification and anaerobic ammonium oxidation. Without nitrogen fixation by cyanobacteria, ocean productivity would gradually decline. Laboratory experiments indicate that nitrogen fixation by cyanobacteria may increase under ocean acidification. But lab results are not easily extrapolated to



**Figure 3:** Satellite image of a cyanobacterial bloom in the Baltic Sea, Foto: Jeff Schmaltz, NASA/MODIS

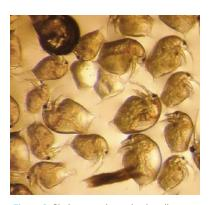
Figure 4: Deployment of the KOSMOS mesocosms at the southern tip of Finland by RV ALKOR, Foto: Ulf Riebesell, GEOMAR

Figure 5: The development in the mesocosms was monitored through daily sampling of over 50 parameters, Foto: Ulf Riebesell, GEOMAR

the natural environment. So the question remains how these responses will play out in the natural ecosystems and what will be the consequences for marine food webs and biogeochemical cycles.

To address these questions a large-scale field experiment was conducted as part of the SOPRAN project (Surface Ocean Processes in the Anthropocene) funded by the German Ministry for Education and Research (BMBF). Coordinated by GEOMAR, a team of 45 scientists from Germany,

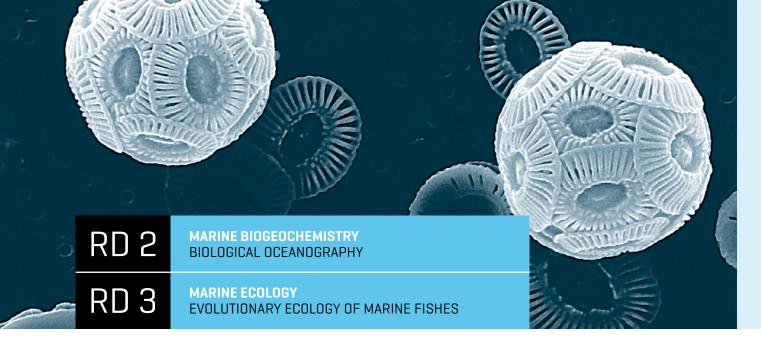
Finland, Sweden, England and the Netherlands set up their instruments at the Tvärminne Zoological Station at the southernmost tip of Finland. GEOMAR's research vessel ALKOR deployed nine of the Kiel Off-shore mesocosms (KOSMOS) in the coastal waters off Tvärminne, bordering the Gotland Sea, an area experiencing regular blooms of cyanobacteria each summer. Each mesocosm captured about 55.000 litres of seawater, thereby enclosing the natural plankton community dwelling in the surface layer. By manipulating the carbonate chemistry inside the mesocosms, a range of CO<sub>2</sub> concentrations was established to simulate the conditions ranging from present day to those projected for mid of next century. Over the course of the seven-week experiment more than 50 parameters were measured daily, covering all aspects from plankton community development and trophic interactions, to carbon, nitrogen and phosphorus cycling, export fluxes and air-sea gas exchange.



**Figure 6:** Cladocerons ingesting bundles of the cyanobacterium *Aphanizomenon*, Foto: Silke Lischka, GEOMAR

Due to unusually cold and windy weather conditions during the summer of 2012, cyanobacteria fell short of producing massive blooms in the Baltic Sea that year. In the mesocosms *Aphanizomenon flos-aquae*, one of the three key species of cyanobacteria in the Baltic Sea, was flourishing while at the same time being heavily grazed upon by the abundant cladoceron *Bosmina longicornis* - so much about the concept of cyanobacteria being despised by zooplankton. By adding molecular nitrogen  $(N_2)$  enriched with the heavy iso-

tope <sup>15</sup>N directly into the mesocosms, we were able to quantify nitrogen fixation by the cyanobacteria and to follow the fate of the newly fixed nitrogen up the food web and through the different pools of nitrogen in the system. This will allow putting the lab-based hypothesis of blue-green algae expanding in the future ocean to a rigorous test in a natural plankton community out in the field. As many of the samples are still in the process of being analysed, it is too early to conclude whether ocean acidification plays in favour of the blue-green algae. The many pieces of this challenging puzzle will be assembled when all groups involved in this study come together again at the data workshop in Kiel in November of this year.



# Evolution at the Sea - Marine Phytoplankton can adapt to Ocean Acidification

Kai T. Lohbeck (RD2,RD3), Ulf Riebesell (RD2) and Thorsten B. H. Reusch (RD3)

On-going ocean acidification represents a major threat for many marine organisms with potential consequences for ecosystem functioning. One question of immediate concern is how sensitive species will respond to these changes. While short-term responses are extensively studied, long-term studies that investigate the potential for evolutionary adaptation are widely neglected. We conducted a 500 generations  $CO_2$  selection experiment using the calcifying microalga Emiliania huxleyi and uncovered a large potential for adaptation to rapidly changing environments in this important phytoplankton species.

Fossil fuel-derived carbon dioxide has a serious impact on global climate but also has a disturbing effect on the oceans - known as "the other  ${\rm CO_2}$  problem". When  ${\rm CO_2}$  dissolves in seawater it forms carbonic acid and results in a drop in pH, a phenomenon dubbed ocean acidification (Caldeira and Wickett 2003).

A wealth of short term experiments has shown that calcifying organisms, such as corals, clams and snails, but also micron size phytoplankton are affected by ocean acidification (Orr et al. 2005). However, the potential for organisms to adapt to acidified oceanic conditions via evolutionary processes has so far been neglected and remains a major unknown when attempting to predict future impacts of ocean acidification on marine life (Riebesell et al. 2009).

Coccolithophores are a case in point. These planktonic microalgae cover their cells with delicate calcite scales and are considered to be among the most productive organisms in the sea (Westbroek et al. 1989). They are sensitive to ocean acidification as their growth and calcification rates decline under increased CO<sub>2</sub> concentrations (Riebesell and Tortell 2011). As coccolithophores reproduce quickly and have large population sizes, they should be particularly prone to respond to ocean change via evolutionary adaptation (Bell and Collins 2008).

To test whether coccolithophores can adapt to ocean acidification we conducted two long-term laboratory selection experEmiliania huxleyi, Foto: Lennart Bach, GEOMAR

Figure 1: Calcifying microalga

iments using the globally important coccolithophore *Emiliania huxleyi* (Fig. 1). Clonal cultures were isolated in Norwegian coastal waters und cultured in the laboratory under ambient (400  $\mu$ atm), medium (1100  $\mu$ atm) and high (2200  $\mu$ atm) levels of CO<sub>2</sub> partial pressure. The ambient-CO<sub>2</sub> treatment was used as control, the medium-CO<sub>2</sub> treatment repre-

sented a level projected for the beginning of the next century and the high-CO<sub>2</sub> treatment served as a proof of principle, representing a sufficiently strong selective force.

One experiment started from replicated populations assembled from equal contributions of six different clones (i.e. different genetic variants) and the other from replicates originating from an arbitrary chosen single clone (i.e. only one genetic variant). The multi-clone experiment was designed to provide the necessary genetic variation that would allow population-level adaptation by clonal selection, whereas in the single-clone experiment adaptation required new mutations to introduce the genetic variation that selection may act on. After about one year, which translates into 500 generations in this rapidly reproducing species, we tested for adaptation to ocean acidification by comparing populations grown under elevated  $\mathrm{CO}_2$  levels with those kept under ambient  $\mathrm{CO}_2$  levels when exposed to ocean acidification conditions (Lohbeck et al. 2012).

With this interdisciplinary approach, combining the expertise from biological oceanography and evolutionary biology we demonstrated for the first time that adaptation to increased  $CO_2$  conditions in a calcifying marine phytoplankton species is possible. In both experiments, *E. huxleyi* populations adapted to elevated  $CO_2$  conditions and showed significantly increased exponential growth rates (in this case a direct measure of Darwinian fitness)

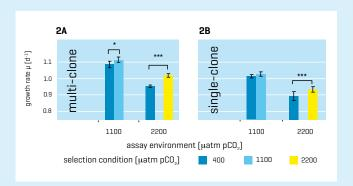
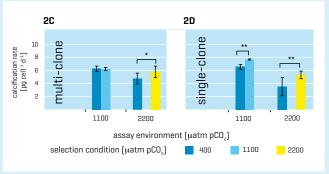


Figure 2: Phenotypic responses after ~500 generations of  $CO_2$  selection in *Emiliania huxleyi*. Replicate cultures (n=5) were initially founded by either six clones (left panels) or a single clone (right panels).



2A,2B,Mean exponential growth rate.

**2C,2D,**Mean production rate of particulate inorganic carbon/calcification rate  $*p \le 0.05$ ; \*\* $p \le 0.01$ ; \*\*\* $p \le 0.001$ ; error bars  $\pm 1$  s.d.].

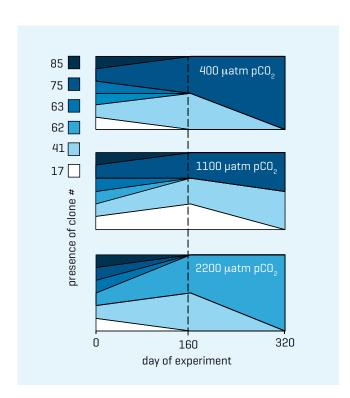


Figure 3: Time course of the presence of *Emiliania huxleyi* clones in the multiclone experiment. All three  $\mathrm{CO}_{z}$  treatments started with the same assemblage of six clones. The presence of individual clones was assessed by polymerase chain reaction of diagnostic alleles at five microsatellite marker loci.

and partly restored calcification rates relative to control populations when tested under ocean acidification conditions (Fig. 2). In the multi-clone experiment we used genetic tools (microsatellite markers) to track changes in genotypic composition of the populations. We could show consistent clonal sorting across all five replicates that resulted in different clones to become dominant in each  $\rm CO_2$  treatment (Fig. 3). We identified genotypic selection as one immediate mechanism of adaptation to elevated  $\rm CO_2$  in the multi-clone experiment. The adaptive response observed in the single-clone experiment suggests that new mutations have occurred and that some of them may be beneficial to cope with increased  $\rm CO_2$  levels.

Given the important role of coccolithophores in ocean productivity and the marine carbon cycle (Westbroek et al. 1989), the swift adaptation processes observed here have the potential to affect food-web dynamics and biogeochemical cycles on climate change-relevant timescales. Our findings emphasize the need to consider evolutionary processes in future studies on the biological consequences of global change. Experimental evolution studies can only reveal the potential for adaptation and therefore need to be further scrutinized against field observations to assess to what extent evolutionary changes observed under laboratory conditions apply in the oceans, where other environmental factors and ecological interactions play along.

#### References

Bell, G., and S. Collins. 2008. Adaptation, extinction and global change. Evol. Appl. 1:3-16.

Caldeira, K., and M. E. Wickett. 2003. Anthropogenic carbon and ocean pH. Nature 425:365–365.

Lohbeck, K. T., et al. 2012. Adaptive evolution of a key phytoplankton species to ocean acidification. Nat. Geosci. 5:346-351.

Orr, J. C., et al. 2005. Anthropogenic ocean acidification over the twenty-first century and its impact on calcifying organisms. Nature 437:681-686.

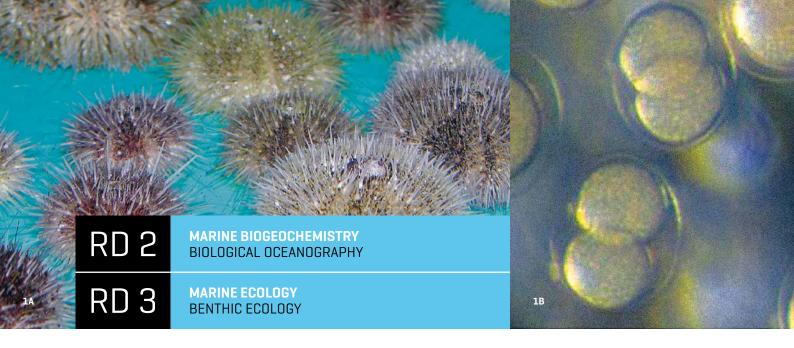
Riebesell, U., et al. 2009. Sensitivities of marine carbon fluxes to ocean change. Proc. Natl. Acad. Sci. U. S. A. 106:20602-20609.

Riebesell, U., and P. D. Tortell. 2011. Effects of ocean acidification on pelagic organisms and ecosystems. Pp. 99-121 in J.-P. Gattuso, Hansson, L., ed. Ocean Acidification. Oxford Univ. Press, Oxford, U.K.

Westbroek, P., et al. 1989. Coccolith Production (Biomineralization) in the Marine Alga *Emiliania huxleyi*. J. Protozool. 36:368-373.

#### **Acknowledgment**

This work was funded by the German Federal Ministry of Education and Research (BMBF) in the framework of the coordinated project BIOACID (Biological Impacts of Ocean Acidification).



### Sea urchin larvae in an acidified ocean

## Understanding physiological tolerance mechanisms in sub-mm sized calcifying organisms

Meike Stumpp (RD3), Marian Y. Hu (RD3), Magdalena A. Gutowska (RD2) and Frank Melzner (RD3)

Using technology developed to study the mammalian kidney, a research team from Kiel and Göteborg was able to measure pH regulatory abilities of very small sea urchin larval stages for the first time. The surprising results indicate that calcifying cells are very good pH regulators, while body fluid pH cannot be controlled in larval stages. Ocean acidification does not impair the ability of larval stages to build a calcium carbonate skeleton, but compromises the larval energy budget, which impacts mortality and delays development – increasing the risk for predation related mortality in the pelagic zone.

Sea urchins are very important components of many coastal ecosystems. The green sea urchin, *Strongylocentrotus droebachiensis*, is a key stone species of temperate regions of the Atlantic and the Pacific Ocean. This species primarily feeds on macroalgae and can control kelp forests, with high populations size of *S. droebachiensis* fluctuating inversely with kelp forest extent in many fjords. Any changes in abundance of this species thus can have far reaching consequences for productive coastal ecosystems (Stumpp et al. 2012a).

Bottom - living adult sea urchins produce larval stages, so called pluteus larvae, that spend several weeks in shallow waters of the open ocean and feed on microalgae and dissolved nutrients. In order to stabilize their long arms, which are the main feeding organs, <0.5 mm small pluteus larvae possess a rigid internal skeleton that is made of high magnesium calcium carbonate. Previous research had demonstrated a high sensitivity of sea urchin larvae to form these skeletal elements (so called 'spicules') when they were exposed to projected scenarios of ocean acidification (Stumpp et al. 2011a,b).

In order to better understand the reasons that underly this high sensitivity, we used laboratory fertilized sea urchin embryos and larvae and investigated the ion regulatory abilities of early life stages. In an interdisciplinary study involving researchers from the Medical Faculty of CAU Kiel and the University of Göteborg in Sweden, we developed novel techniques to

directly measure in vivo pH in the body cavity and in the skeleton forming cells (primary mesenchyme cells, PMCs). Using extremely thin pH microelectrodes, we were able to demonstrate that the pH in the body cavity passively follows that of the surrounding seawater, indicating a very limited pH regulatory capacity. Ocean acidification thus leads to very strong changes in the fluid that surrounds the calcifying cells of the larval body.

On the other hand, we could demonstrate that PMCs are able to maintain a constant pH even when the surrounding fluid is acidified. We accomplished this by 'loading' PMCs with a fluorescent, pH sensitive chemical dye (BCECF). Changes in pH in cells could then be monitored using a microscope while the cells were exposed to changes in seawater pH in a water bath. As initial CaCO<sub>3</sub> production is located within vesicles in PMCs, we believe that successful calcification is enabled by the strong pH and ion regulatory capacity of these cells. However, the decreased body cavity pH under acidified conditions probably compromises the larval energy budget, as protons generated during calcification within PMCs have

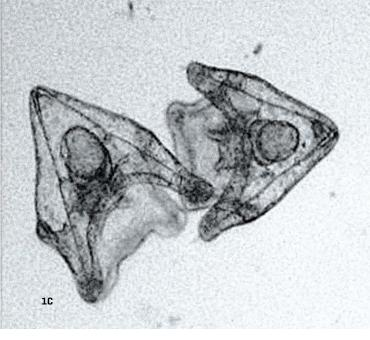


Figure 1-3: Sea urchin life cycle. Adult Green sea urchin, ca. 5-6 cm diameter [1A]; laboratory fertilized embryo, 2 -cell stage, ca. 80 μm diameter(1B); pluteus larvae raised in the laboratory, ca. 0.3 mm long [1C]. Images: F. Melzner, M. Stumpp, GEOMAR

to be excreted against a steeper pH gradient (Stumpp et al. 2012b).

In order to test this hypothesis, we determined larval energy consumption and energy uptake. Oxygen consumption rates of pluteus larvae were determined using micro - respirometer chambers and oxygen optode technology, while feeding rates were monitored separately. We could demonstrate that high CO2 induced elevations in metabolic rate, while feeding rates remained constant. This led to a compromised energy budget, with less energy being available for growth and calcification processes (Stumpp et al. 2011a). Hence, it appears that sea urchin larvae can maintain their ability to calcify even in strongly acidified seawater. The observed reductions in growth and calcification were due to energy budget re-allocation, which could be caused by higher costs for cellular pH regulation. Changes in mRNA expression of certain ion transport proteins support this hypothesis (Stumpp et al. 2011b).

Reduced developmental speed of larvae can translate into increased mortality, as predation rates are very high in the open ocean. As mortality of larval stages is already very high (>90%), additional changes in mortality could affect populations and function of kelp ecosystems. Future research efforts needs to address the capacity for adaptation to a changing abiotic environment in ecologically important echinoderm species.

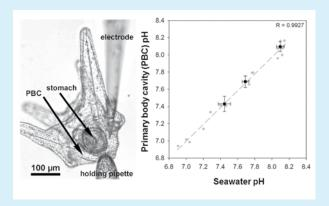


Figure 4: pH measurements in pluteus larvae. Left: pluteus larva in a water bath under a microscope, held in place with a holding pipette. The pH electrode is gently inserted into the primary body cavity [PBC] to measure body fluid pH; right: body fluid pH in relation to seawater pH in pluteus larvae. Acute exposure to low pH (grey) vs. chronic exposure to low pH [black]. Image, figure: M. Stumpp, GEOMAR

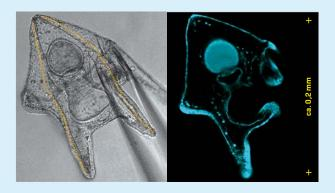


Figure 5: Sea urchin larva [ca. 0.3 mm] under the confocal microscope [left, spicules marked in yellow]. The larva is held under the microscope with a pipette in a water bath so that the liquid in the water bath is continuously exchanged. The same larva stained with a pH sensitive dye [right]. The calcifying cells [PMCs] are visible as green spots along the spicules in the arms. Changes in PMC pH cause a difference in fluorescence that can be quantified using a microscope and image analysis software. Images: M.A. Gutowska, GEOMAR

#### References

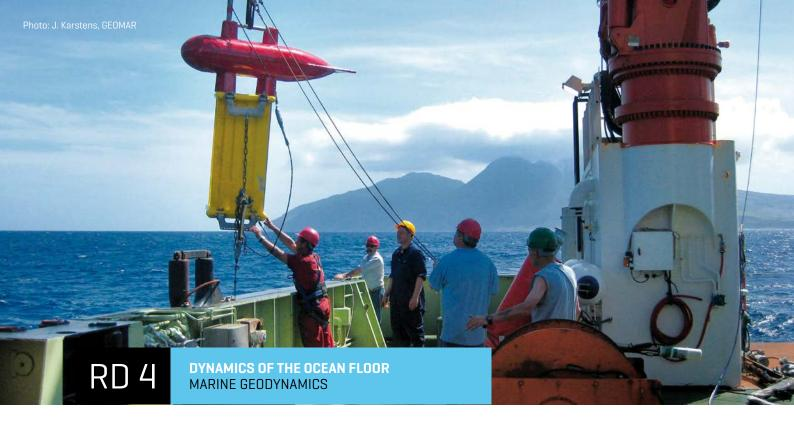
Stumpp, M., Wren, J., Melzner, F., Thorndyke, M.C., Dupont, S. [2011a]. CO<sub>2</sub> induced acidification impacts sea urchin larval development I: elevated metabolic rates decrease scope for growth and induce developmental delay. Comparative Biochemistry and Physiology A 160:331-340.

Stumpp, M., Dupont, S., Thorndyke, M.C., Melzner, F. [2011b].  $\rm CO_2$  induced acidification impacts sea urchin larval development II: developmental delay influences the interpretation of gene expression patterns. Comparative Biochemistry and Physiology A 160:320-330.

Stumpp, M., Trübenbach, K., Brennecke, D., Hu, M.Y., Melzner, F. [2012a]. Ressource allocation and extracellular acid-base status in the sea urchin *Strongylocentrotus droebachiensis* in response to seawater acidification. Aquatic Toxicology 110-111:194-207.

Stumpp, M., Hu, M.Y., Melzner, F., Gutowska, M.A., Dorey, N., Himmerkus, N., Holtmann, W., Dupont, S.T., Thorndyke, M.C., Bleich, M. (2012b). Acidified seawater impacts sea urchin larvae pH regulatory systems relevant for calcification. Proceedings of the National Academy of Sciences of the USA 109:18192-18197.





# New insights into fluid flow in Hydrate Ridge, Oregon

#### Christian Berndt, Gareth Crutchley, Nathan Bangs and Matt Hornbach

After many marine geophysical and geological expeditions including two ocean drilling program legs GEOMAR and American collaborators revisited Hydrate Ridge off Oregon in 2008 to collect a high-resolution 3D seismic data set. The results have now been published in two GEOLOGY articles and one Earth and Planetary Science Letter. They reflect the change of our understanding of sedimentary fluid flow systems derived from the new 3D seismic data showing that gas can migrate about ten times faster in the subsurface than previously thought, that there must be far more hydrate in the system than predicted based on 2D seismic data and drilling results, and that the presence of gas has a profound effect on effective permeability. In fact, its presence can generate sufficiently high excess pore pressures that hydro-fracturing and focusing of fluid flow occurs. Our results explain the observed location of cold-vent ecosystems on Hydrate Ridge and provide information on the temporal variability of gas emanations.

Hydrate Ridge is located 90 km west of Oregon's coast. It is an anticlinal structure in the accretionary prism of the Cascadia subduction zone. The widespread occurrence of cold seeps, methane gas, and gas hydrates are the result of an up to 3.5 km thick incoming sedimentary sequence of continental-derived turbidites and hemipelagic mud overlain by Quaternary fans from the Columbia River and the Straits of Juan de Fuca. Hydrate Ridge is one of the best-studied hydrate provinces in the world.

In 2008 we collected a 3D seismic data set, which was designed to improve spatial resolution by towing streamers with a narrow, 12.5 m line spacing and 2 GI guns as a seismic source. With

the new 3-D seismic data, we imaged strata and structures beneath the southern summit of Hydrate Ridge in unprecedented detail to determine the geological processes controlling the style of focused fluid flow, which is the basis for a methane seep at the seafloor. This seep hosts chemosynthetic ecosystems and releases significant amounts of carbon into the ocean.

The seep is inherently dynamic and flux varies greatly in magnitude and even flow direction over short time periods (hours-to-days), often tidally-driven (Tryon et al., 2002). But it was unclear if flux changes at vents occur on the order of the life-cycle of various species within chemosynthetic communities (month, years, to decades Leifer et al., 2004) and thus impact their sustainability. Comparing the 2008 data to 3D seismic data acquired in 2000 we are able to demonstrate that Hydrate Ridge has undergone significant

reduction of methane flow and complete interruptions in just the past few years (Bangs et al., 2011). In the subsurface, below a methane hydrate layer, free gas appears to be migrating toward the vent, but currently there is accumulating gas that is unable to reach the seafloor through the gas hydrate layer. At the same time, abundant authigenic carbonates show that the system has been active for several thousands of years. Thus, it is likely that activity has been intermittent because gas hydrates that clog the vertical flow pathways feeding the seafloor vent. It is likely that pressure build-up in the subsurface will ultimately trigger hydrofracturing that may revive fluid-flow to the seafloor. The nature of this mechanism implies regular recurring

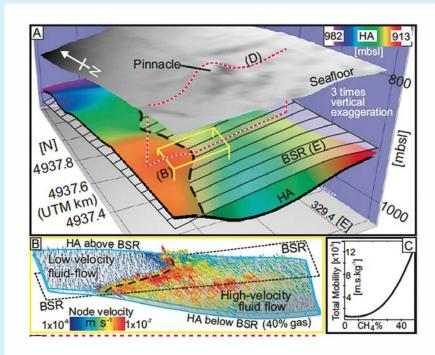


Figure 1: a) At the intersection of the gas hydrate stability zone (BSR) and a gas transporting ash layer (HA) overpressure builds up due to increased flow velocities (b). These are primarily the result of the increased fluid mobility due to high gas concentrations imaged by the 3D seismic data and confirmed by drilling results (c). The Pinnacle structure at the seafloor is a carbonate reef that is caused by carbonate precipitation due to biological activity at the seep site (modified from Crutchley et al., 2013).

flow interruptions and methane flux changes that threaten the viability of chemosynthetic life, but simultaneously and enigmatically sustains it.

Numerical fluid flow simulations reveal the influence of free gas within a stratigraphic unit known as Horizon A, beneath the base of gas hydrate stability (BGHS). Free gas within Horizon A increases the total mobility of the composite water-gas fluid, resulting in high fluid flux that accumulates at the intersection between Horizon A and the BGHS (Crutchley et al., 2013). This intersection controls the development of fluid overpressure

at the BGHS, and together with a well-defined network of faults, reveals the link between the gas hydrate system at depth and methane seepage at the surface.

Gas hydrates represent a potentially enormous unconventional methane resource that may play a critical role in climate change and ocean acidification; however, it remains unclear how much hydrate exists. Analysis of the 2008 data reveals where fluids migrate in three dimensions across a continental margin and is used to quantify hydrate with meter-scale horizontal resolutions (Hornbach et al., 2012). Our study, suggests that heat flow and hydrate concentrations are coupled, and that 3-D thermal analysis can be used to constrain hydrate and fluid flow in 3-D seismic data. Hydrate estimates using this technique are consistent with 1D drilling results, but reveal large, previously unrecognized swaths of hydrate-rich sediments that have gone undetected due to spatially limited drilling and sampling techniques used in the

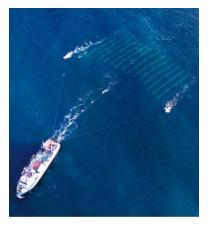


Figure 2: aerial view of a P-Cable system deployed from a research vessel. Photo: Geometrics Inc.

past studies. The 3-D analysis suggests the previous hydrate estimates based on drilling at this site are low by a factor of approximately three.

The wealth of insights gained from a 10 day-deployment of the P-Cable 3D seismic system in an area that had been the subject of many marine geological expeditions previously and was thought to be well understood, illustrates impressively the power of 3D seismic imaging.

#### References

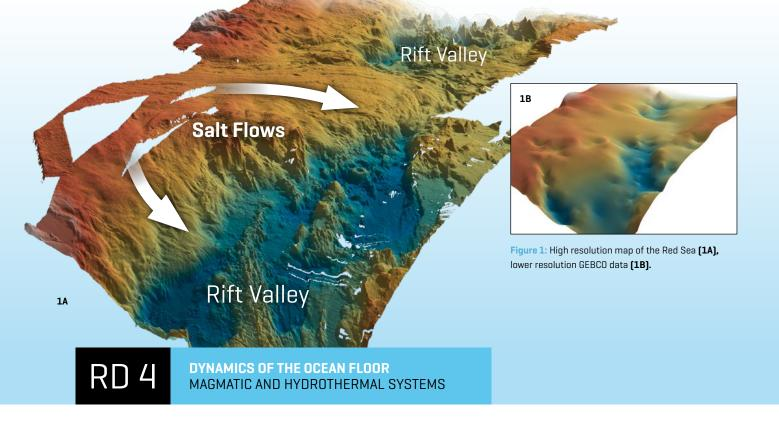
Bangs, N. L. B., Hornbach, M. J. und Berndt, C. [2011] The mechanics of intermittent methane venting at South Hydrate Ridge inferred from 4D seismic surveying Earth and Planetary Science Letters, 310 [1-2]. pp. 105-112. DOI 10.1016/j.epsl.2011.06.022.

Crutchley, G. J., Berndt, C., Geiger, S., Klaeschen, D., Papenberg, C., Klaucke, I., Hornbach, M. J., Bangs, N. L. B. und Maier, C. [Im Druck / Accepted] Drivers of focused fluid flow and methane seepage at South Hydrate Ridge, offshore Oregon Geology.

Hornbach, M., Bangs, N. und Berndt, C. (2012) Vast quantities of methane hydrate detected via 3D thermal modeling Geology, 40 (3). pp. 227-230. DOI 10.1130/G32635.1.

Leifer, I., Boles, J.R., Luyendyk, B.P., Clark, J.F., [2004], "Transient discharges from marine hydrocarbon seeps, spatial and temporal variablility," Environmental Geology, 46, 1038-1052.

Tryon, M. D. K. M. Brown, M. E. Torres, Fluid and chemical flux in and out of sediments hosting methane hydrate deposits on Hydrate Ridge, OR, II: Hydrological processes, EPSL, 201, 541-557, 2002.



## **Opening up the Red Sea**

#### Nico Augustin, Colin Devey

The splitting of a continent to form an ocean basin is one of the basic processes of plate tectonics and fundamental to all of ocean sciences. One of the few places on Eath where this process is occurring today is in the Red Sea, where the Arabian Peninsula is separating from Africa. For many years, research on the opening of the Red Sea was at a stand-still. As part of a four year joint project with the King Abdulaziz University (KAU) in Jeddah, scientists from Geomar have been using a combination of modern multibeam mapping and targetted sampling to study this continent-scale crack in Earth's surface. The results are set to radically change our ideas of how new oceans form.



Figure 2: Research Vessel PELAGIA in the Red Sea. Foto: N. Augustin, GEOMAR

Although it is clear that a period of continental thinning and rifting precedes the final split, there are at present two competing theories for how the split actually occurs. One theory is that a long length of rifted continental crust separates geologically instantaneously, leading to synchronous creation of new ocean floor over a wide region. The second theory, popular up to present for the Red Sea, is that new seafloor is being formed at various points along the rift but that these points are separated by still-intact continental crust. Although the new Geomar-KAU results are still being debated with scientific colleagues, a first interpretation seems to show that the Red Sea behaves just like other opening oceans and that no seafloor "points" are in fact present. The reason for the confusion is salt! During the thinning and rifting phase of Red Sea opening, the area was covered by a shallow sea which dried out repeatedly, leading to thick salt deposits being formed. Over geological time, salt flows like a glacier. The new high-resolution maps show that, as the Arabian continent split and new seafloor was formed, the kilometer-thick salt deposits on the margins flowed over the new ocean crust. The extent of this flow was not identical everywhere, leading to

small areas of the ocean crust still peeking out from under their "salt blanket".

If this interpretation is correct, the implications are profound. Firstly, there is truly a single mechanism by which continents split, leading to the question of what controls how long the new section of seafloor is. Secondly, we do not know how much ocean crust is covered by salt along the whole Red Sea margin, making the time of Red Sea opening (and so the separation of Africa and Arabia) questionable.

#### References

Augustin, N., Devey, C. W., Feldens, P., van der Zwan, F. M., Bantan, R. and Kwasnitschka, T. (2012) The transition from rifting to spreading in the Red Sea: No sign of discrete spreading nodes? Abstract OS11E-07 presented at 2012 Fall Meeting, AGU, San Francisco, Calif., 3-7 Dec.

Augustin, N., Devey, C. W., Bantan, R., van der Zwan, F. M., Feldens, P. and Kwasnitschka, T. (2012) Hatiba to Port Sudan Deep (Red Sea): Imaging a growing Ocean, Goldschmidt Conference 2012, 24.-29.06.2012, Montreal, Canada.

van der Zwan, F. M., Augustin, N., Devey, C. W., Bantan, R., Kwasnitschka, T. [2013]: New insights into volcanism and tectonics in the Red Sea Rift. Geophysical Research Abstracts, 15, EGU2013-7188

